Proceedings of ASME Turbo Expo 2011
GT2011
June 6-10, 2011, Vancouver, British Columbia, Canada

GT2011-45358

VALIDATION OF CONJUGATE HEAT TRANSFER PREDICTIONS ON LABYRINTH SEALS AND NOVEL DESIGNS FOR IMPROVED COMPONENT LIFETIME

Dominik Born, Kurt Heiniger
Institute for Thermo- and Fluid Engineering, FHNW Windisch

Giorgio Zanazzi, Thomas Mokulys, Patrick Grossmann, Luca Ripamonti, Michael Sell
Alstom Power
Baden, Switzerland

ABSTRACT

Cyclic lifetime assessment of steam turbine components has become increasingly important for several reasons. In the last years and decades the nominal steam temperatures and pressures were further increased to improve cycle efficiency. In addition, the market constantly demands increased flexibility and reliability for given lifetime exploiting the limits of the existing materials.

A number of components in a steam turbine are critical in the focus of lifetime predictions such as the rotor and front stage blades, the inner casing and the area of labyrinth seals connected to the life steam. For this reason, it becomes extremely important to rely on accurate predictions of local temperatures and heat-transfer-coefficients of components in the steam path.

The content of this paper aims on the validation of the numerical tools based on CHT (conjugate heat transfer) approach against experimental data of a labyrinth seal regarding discharge coefficients and measured heat transfer coefficients.

Furthermore, a real steam turbine application has been optimized in design and operation to improve lifetime. The improved prediction of temperature and heat transfer allowed novel designs of labyrinth seals of a single flow high-pressure turbine and a combined intermediate and low-pressure turbine, which helped to strongly increase the component lifetime of a steam turbine rotor by more than 100%.

INTRODUCTION

Modern Steam Turbine Power plants show increasing firing and turbine inlet temperatures to improve the cycle efficiency and reduce CO_2 production. Among others Alstom continuously develops in this respect better and more advanced steam turbines with flexible operation and accurate prediction of lifetime.

The current power market demands, to be competitive, more flexible operation, with faster start-up and load change. Increasing the flexibility and performance of the power plants and, on the other side, elongating the life and reliability, reduces the number of maintenance tasks and cost, for both single flow high-pressure turbine and combined intermediate and low-pressure turbine.

One of the technically challenging problems is the design of the inlet flow path to the turbine, which features a so-called piston and labyrinth seal. This area of the turbine has the highest temperatures and high mechanical stresses. Additionally it features leakage flows that lower the performance of the turbine. There is a highly complex interaction of heat transfer between leakage steam flow and rotor material.

There are three possible ways to predict temperatures and heat transfer in labyrinth seals. The most important is still the application of 1-dimensional correlations, the second would be to rely on experimental tests and the third would be to simulate the labyrinth seals with numerical tools.

One-dimensional correlations are well-established and have been applied in the design of steam turbines up to the current date. Trutnovsky und Komotori ([15], 1981) summarize the most important experimental results and theories in their collection.

Half-empirical correlations are an easy method of describing the discharge through labyrinth-seals. An often used and practical method is the consideration of the labyrinth flow as a series of orifice type restrictions. Many attempts have been made in describing the leakage losses through labyrinth seals with this method. Early attempts arise from *Stodola ([14]*, *1927)*, *Egli (*[3], *1935)*, *Kearton und Keh ([7]*, *1952), Jones ([6]*, *1952) and Komotori ([8]*, *1961).*

Egli ([3], 1935) gives a half-empirically determined treatment of a sharp-edged orifice. It is also shown how to consider the effect of transported kinetic energy from one throttling into the next.

Jones ([6], 1952) did a large number of tests of complete seals and constructed from the results a graphical method to estimate the discharge. The numbers of lands in gland, pitch to clearance ratio, as well as the pressure ratio, were considered. This method is also nowadays an often-used one.

Komotori ([8], 1961) did detailed investigations concerning the effect of the labyrinth geometry on the discharge. In further researches *Komotori und Miyake ([9], 1977)* studied experimentally the leakage characteristic of straight through labyrinth seal with high rotating motion.

Heat transfer itself can be correlated from models that describe the discharge coefficient, but these models include very often large conservatism for lifetime prediction as the detailed internal heat transfer remains very complex and cannot be sufficiently approximated with simple analytical models. For this reason, experiments have been created to accurately measure the heat transfer.

Especially at the technical University of Karlsruhe a number of experiments in the field of labyrinth flows have been conducted in the last thirty years. *Waschka ([16]*, *1991)* carried out comprehensive measurements of heat transfer and leakage loss in compressible flows in labyrinth seal with different designs and clearances. Detailed temperature measurements allowed the determination of local heat transfer coefficients for a see-through type of labyrinth seal. The advantage of the experiments is that the measurements are usually beyond doubt for a given case. The limitations of experiments being that test conditions may differ from the real turbine conditions. Also in simulating steam turbines it is practically impossible to generate a test rig that has sufficient Reynolds number. It is also very difficult to extrapolate an aerodynamic behavior from a test result if a geometric parameter is changed, e.g. the radial clearance of the seal.

Especially numerical methods to predict the aerodynamics of labyrinth seals have especially gained in relevance recently, due to the development of high performance computers. Numerical tools can be relatively easily adapted to the correct boundary conditions and geometry of a seal. This helps fill the gap between experiments and real design.

Early investigations regarding the numerical analysis of the flow characteristic of seals were obtained by *Rhode und Sobolik ([11]*, *1986)*, where the solution domain was limited to one chamber and periodic flow conditions were assumed.

Scherer ([13], *1994)* simulated a complete labyrinth seal configuration. Because of deficits of experimental data and the limited computer systems, a validation of the simulation results, especially the local heat transfer, was difficult.

Heat transfer remains a challenging topic for any simulation especially for labyrinth seals. One important topic of this paper is the validation of the flow characteristic and heat transfer results in a typical labyrinth seal with state-of-the-art simulation-codes, in our case the ANSYS CFX 12.1 code. With the aim of validating the simulated results, a numerical model of the test rig of *Waschka ([16]*, *1991)* was developed. With this, a comparison of simulation results with measurements considering conjugate heat transfer was possible. From the test rig, which was operated with air and critical pressure ratios, temperature, discharge coefficients and pressure distribution, as well as local heat transfer coefficients, were available and could be used to validate the numerical tool.

In the second part of this paper, the methodology of conjugate heat transfer calculations has been applied to a conventional and an optimized design of a labyrinth seal in a real steam turbine application. The accurate predictions of temperature and heat transfer inside the labyrinth seal were used to perform a transient thermal structural analysis with an in-house tool of Alstom to assess the relative improvement in lifetime of the new steam turbine design. The methodology of the lifetime assessment has been presented by *Ehrsam* [4].

NOMENCLATURE

Variables

A	area, m^2
c_D	Discharge Coefficent
c_p	spec heat capacity (const. pressure), J/(kg K)
f	recovery factor
L	length, m (cp. Fig. 1)
$\dot{m}$	mass flow, kg/s

$\dot{q}$	spec. heat flux, W/m^2
$\dot{Q}$	heat flux, W
$\dot{Q}_{ideal}$	ideal flow function, $\sqrt{(kg \cdot K)/J}$
r	radius, m
R	specific gas constant, J/(kg K)
Re	Reynolds Number
s	Gap, m
Sf	Swirl factor
T	temperature, °C
$\overline{T}_S$	area average of the temperature on entire rotor and stator surface, °C
Ta	Taylor Number
u	velocity, m/s
WS-SD	Warm Start – Shut Down Cycle
y^+	dimensionless wall distance
α	local heat transfer coefficient, W/(m^2 K)
κ	isentropic coefficient
λ	thermal conductivity, W/(m K)
μ	dynamic viscosity, kg/(m s)
ν	kinematic viscosity, m^2/s
ρ	density, kg/m^3

Subscripts

ax	axial direction
cfd	simulated value
ci	circumferential direction
crit	critical value
CS	cool surface on cooling side
ft	Fin tip
G	gas
gap	Gap
HS	hot Surface on flow side, in the labyrinth
ideal	ideal conditions
M	metal
meas	measured value
0	at the inlet of the labyrinth
point wise	point wise on measurement position
rec	recovery
ref	reference
sh	Shaft
S	Surface
tot	total
x	x-direction, axial
∞	at the outlet of the labyrinth

VALIDATION WITH EXPERIMENTAL DATA

Description of the test-rig

A test facility from the Technical University of Karlsruhe has been utilized for validation purposes of the numerical model. The test-rig was developed and used by Waschka [16] to investigate the influence of high rotating speeds on heat transfer and discharge coefficients in labyrinth seals. The following descriptions have been taken from this work:

The test section is of a "see through" labyrinth type, as it consists of a smooth stator-part and an inner rotating part with six sealing strips (see Fig. 1). The fins have a diameter of 250 mm, pitch 12 mm, height 10.5 mm and a thickness of 2.5 mm. The radial clearance measures 1 mm. The rotor is driven by an electric engine with max. 3000 rpm in connection with a flat belt drive (ratio 1:7). An electrical heater can be used to heat up the supplied air to 400°C. A compressor with a maximum mass flow of 0.5 kg/s supplies the air. Downstream of the labyrinth the air exits in a diffuser whose end is exposed to ambient pressure.

For heat transfer measurements, the rotor and stator part can be cooled. The stator is cooled with water and the rotor with air.

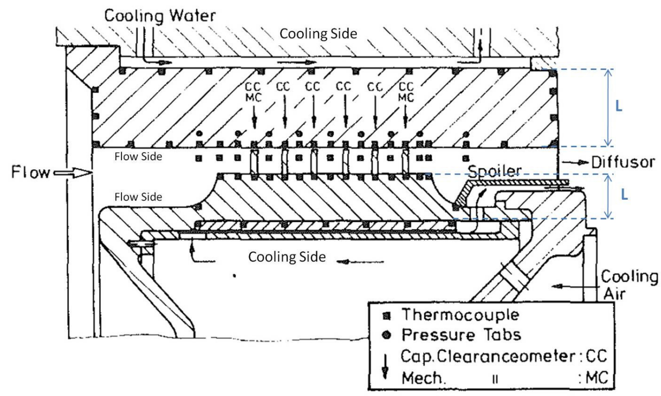

Fig. 1 Test-Section and Instrumentation of the Labyrinth from Waschka ([15], 1991)

The temperature distribution of the surfaces on the cooling- and flow-side of stator and rotor can be obtained with Thermocouples NiCr-Ni (Type J, diameter 0.5 mm). The gas temperature is measured in the middle of every chamber on the height of the fins. In front of the test-section is a calming chamber, which provides an approximately axial flow into the labyrinth. Temperature measurements in three different cross sections in this chamber were used to determine the inlet gas temperature. Furthermore the mass flow is measured with orifice meters. Finally pressure taps in the stator allow the capture of the pressure distribution inside the seal.

A detailed explanation of the test-facility and the instrumentation can be found in Waschka [16].

Theory of Definitions

Two different definitions of the *local heat transfer coefficients* are used. One definition is used in the validation stage, in which the simulation data is compared with measurements and the other will be used during the sensitivity analysis concerning the mesh discretization. The differences between the two definitions are the used specific heat flux and the reference temperature in the gas.

With the aim to compare the simulation results with measurement data, local heat transfer coefficients are derived from equation (1). That definition is subscripted with the index *ref1* and will be used in the *validation stage*.

$$\alpha_{ref1} = \frac{\dot{q}_{ref1}}{(T_{G\_ref1} - T_S)} \tag{1}$$

Because the validation is bound to the measurements, a separate definition for the heat flux and the reference gas temperatures has to be used. That means for the direct comparison of the simulated data with measurement, the *heat flux* is defined with equation (2)

$$\dot{q}_{ref1} = -\lambda_M \cdot \frac{(T_{HS} - T_{CS})}{L} \tag{2}$$

where the temperature gradient in the solid domains between the flow- and cooling side is used. The definition of L can be seen in Fig. 1. This definition is not equivalent to the real heat fluxes, because it neglects the axial temperature distribution. In reality there is a variation in the temperature distribution along the fluid domain. This definition will only be used to compare consistently the measurements with simulation results.

The *reference gas temperature* T_{G_ref1} were chosen point wise at the measurement positions. The measured temperature is a *recovery temperature* with a recovery factor f of 0.8 as shown in eq. (3).

$$T_{G\_ref1} = T_{G\_rec} = T_{stat} + f \cdot \frac{u^2}{2 \cdot c_P} \tag{3}$$

As mentioned before the reference variables to determine local heat transfer coefficients will be changed to check the mesh sensitivity of the results. The heat transfer coefficient will then be declared with the index *ref2*.

$$\alpha_{ref2} = \frac{\dot{q}_{ref2}}{(T_{G\_ref2} - T_S)} \tag{4}$$

In this case, the heat flux is directly extrapolated by the solver is considered.

Furthermore the definition of the point wise *reference gas temperature* will be changed. In the sensitivity analysis the recovery temperature for each area cross-section will be mass flow averaged (see eq. (6)).

$$T_{G\_ref2} = \frac{\int_{A(x)} \rho \cdot |u| \cdot T_{G\_rec} \cdot dA}{\int_{A(x)} \rho \cdot |u| \cdot dA} \tag{6}$$

the Nusselt-Number serves for the *global heat transfer* analysis. The Nu-Number is defined in eq. (7).

$$Nu = \frac{\overline{\alpha} \cdot 2 \cdot s}{\lambda_G} \tag{7}$$

The double gap width is used as characteristic length. The parameter s defines the nominal gap width of 1 mm. Moreover a mean heat transfer coefficient, either from the rotor, or from the stator leads to global information (see eq. (8)).

$$\overline{\alpha} = \frac{\dot{Q}_{tot}}{A_{tot}(T_{G\_ref2} - \overline{T}_S|_{area\_average})} \tag{8}$$

The *rotational effect* is described with the *swirl factor* Sf. The swirl factor is defined as the relation between the impulses in the circumferential direction to the axial impulse. This is equivalent to the relation of the Reynolds-Numbers in these two directions.

$$Sf = \frac{\mathrm{Re}_{ci}}{\mathrm{Re}_{ax}} \tag{9}$$

with

$$\mathrm{Re}_{ax} = \frac{\dot{m}}{\mu \cdot \pi \cdot r_{ft}} \tag{10}$$

and

$$\mathrm{Re}_{ci} = \frac{u_{Sh} \cdot 2 \cdot s}{\upsilon} \tag{11}$$

The Taylor-Number is an additional parameter, which was also used to describe the influence of rotation.

$$Ta = \frac{u_{sh} \cdot 2s}{\upsilon} \cdot \sqrt{\frac{s}{r_{sh}}} \tag{12}$$

To describe the mass flow through the labyrinth seal, the discharge coefficient was used. This dimensionless coefficient is defined with eq (13).

$$c_D = \frac{\dot{m}_{meas}}{\dot{m}_{ideal}} \tag{13}$$

The ideal mass flow is defined as the mass flow through an ideal nozzle with the same entire pressure ratio and the same cross section area as the gap in the labyrinth.

$$\dot{m}_{ideal} = \frac{\dot{Q}_{ideal} \cdot A_{gap} \cdot p_0}{\sqrt{T_0}} \tag{14}$$

In the case of subcritical flow conditions the ideal flow function is defined with eq. (15)

$$\dot{Q}_{ideal} = (\frac{p_\infty}{p_0})^{\frac{1}{\kappa}} \cdot \sqrt{\frac{2\kappa}{R \cdot (\kappa - 1)} \cdot \left[1 - \left(\frac{p_\infty}{p_0}\right)^{\frac{\kappa-1}{\kappa}}\right]} \tag{15}$$

If the pressure ratio is supercritical, then the value of the ideal flow function can be defined with the maximum value at

$$\left(\frac{p_\infty}{p_0}\right)_{crit} = \cdot \left(\frac{2}{\kappa + 1}\right)^{\frac{\kappa}{\kappa-1}} \tag{16}$$

<u>Description of the CFD-Model</u>

ANSYS CFX 12.1 was used as simulation software to simulate the physical phenomena. The numerical model contains three *domains*, which are visible in Fig. 2. Those are the solid domains of *Stator* and *Rotor* and the fluid domain called *Fluid*. By the use of these three domains it was possible to simulate the entire conjugate heat transfer phenomena. The meshes of the domains are connected with a General Grid Interface (GGI). Because of the symmetry of the flow, the model is built up over 1° in circumferential direction with two cells in this direction. *Rotational periodic* interfaces are used as boundary conditions. The rotational symmetry of the flow field was proven by measurements of *Waschka ([16], 1991).*

More detailed information about the domain modeling can be seen in Table 1.

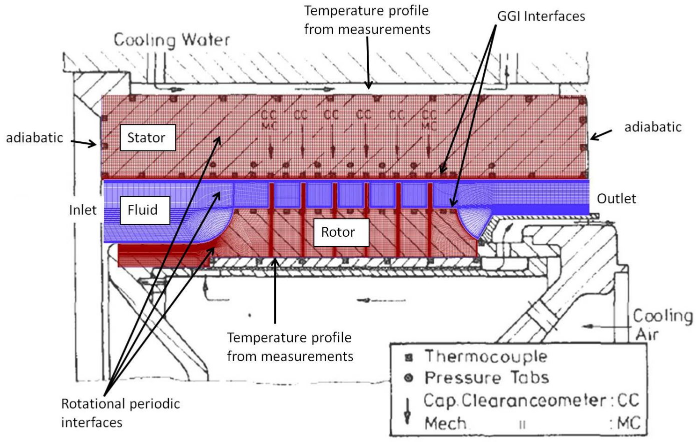

Fig. 2 System Boundary and domains of the numerical model

The *pressure ratio* over the test section was used for the inlet and outlet boundary conditions. It is defined as the relation between the Total pressure at the Inlet and the static pressure downstream of the last fin. The air at the inlet has a total temperature of 433 K, a total pressure of 1.65 bar and a turbulence intensity of 5 %. At the outlet the air is exposed to ambient static pressure of 1.013 bar. The behavior of the flow was assumed as *steady state*.

Domain	Option/Value
Fluid	- Type: Fluid Continuous - Domain Motion: Stationary - Material: Air as an ideal gas; Dynamic viscosity as a function of temperature with Sutherland correlation - Turbulence Model: SST (Shear Stress Transport) - Heat Transfer: Total Energy (incl. Viscous Work)
Stator/Rotor	-Type: Solid Continuous -Domain Motion: Stationary (Stator) Rotating with 5020 rpm (Rotor) -Material: X20Cr13 Steel (WNr. 1.4021) -Heat Transfer: Thermal Energy

Table 1 Domain details of the numerical model

On the *Solid Domains Rotor* and *Stator* temperature profiles of measurement data from *Waschka ([16], 1991)* were used on the cooling side. Remaining system boundaries are declared as adiabatic walls.

In the context of *mesh sensitivity* analysis, three different kinds of fluid discretization and two different solid discretizations had been developed (see Fig. 3). Due to the simple geometry, it was possible to use a structured hexahedron mesh. The mesh has been created based upon three quality aspects. Those are the mesh angle, 3x3 determinants and the aspect ratio.

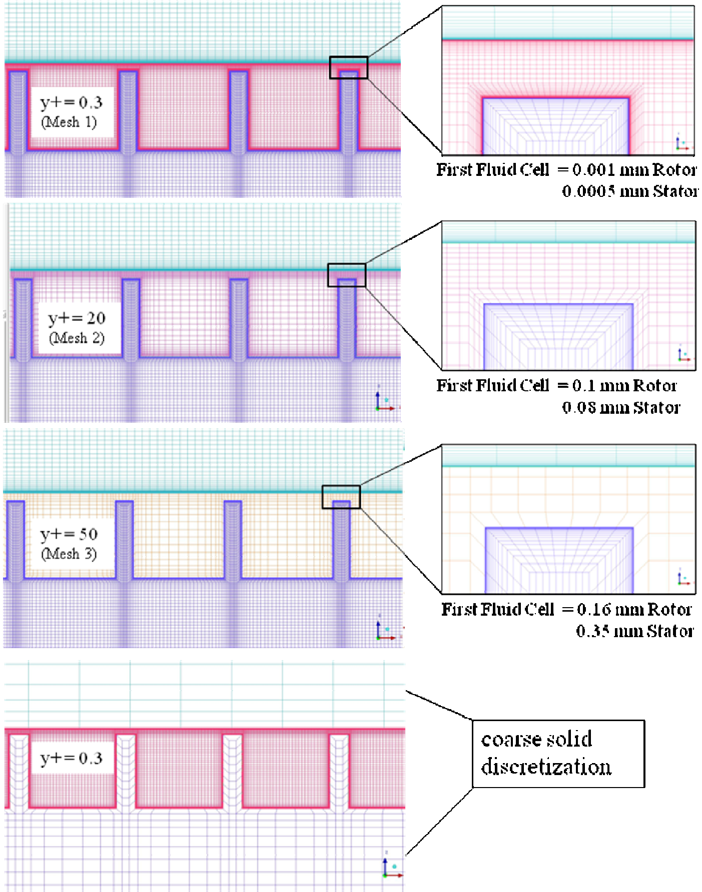

Fig. 3 Combination of the different mesh discretizations

Fig. 4 illustrates the local near wall modeling of the stator and rotor parts of *Mesh 1*. In the case of the stator it is quite constant. The carry over effect causes this result. The y+ on the rotor deviates between the values 0.05 and 0.5.

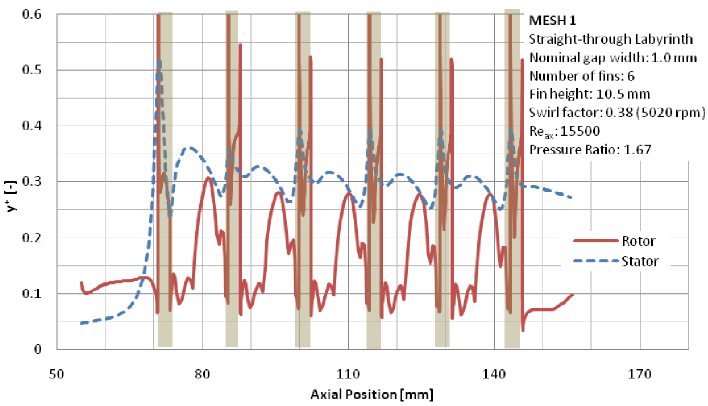

Fig. 4 Local Wall Distance of Stator and Rotor of Mesh 1

Comparison with Experiments

Beside the aim of validating heat transfer values, the first comparisons will focus on the global discharge parameters of the labyrinth seal. Fig. 5 shows the comparison of simulation data with experiments. Generally, one can state the differences between model and experiment range in the order of 3 %. One can judge that the numerical model is able to reproduce the discharge through the seal quite accurately. From the test data, one can see that the discharge coefficient becomes independent from the rotational speed if the Reynolds-Number is higher than about 14000. This is also reflected correctly in the numerical data. The reason for this is that upon this Reynolds number the axial flow impulse is more dominant as the impulse in circumferential direction and frictional effects become less dominant. The swirl factor (see eq. 9) is in this case less than one. Especially in see-through type labyrinths, this causes a rotation-independent discharge.

For the analysis of heat transfer, the operating conditions of Table 2 have been chosen.

As per the definitions presented in eq. 1 and 2, the temperature distributions in the gas and on the rotor/stator surfaces determine the heat transfer coefficient. For this reason the gas temperature and the surface temperatures of the numerical simulations are compared first with measurements.

Option	Experimental Test Rig
Reynolds-Zahl Re_{ax}	15500
Swirl factor Sf	0.38
Pressure Ratio π	1.67
Axial Mach Number M_{ax}	0.63

Table 2 Details of the flow conditions

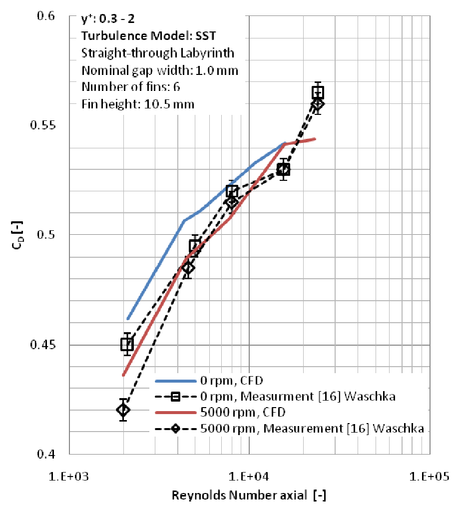

Fig. 5 Discharge coefficient of measurements and CFD

Fig. 6 shows the comparison of the *recovery gas temperature* for the case of the finest mesh 1. The simulation values turn out to be slightly below the test data, especially in the middle of the test section. The maximum difference between simulation and locally measured temperatures in the labyrinth is here about 3 °C. The positions of the test data are in the middle of each chamber on the height of the fins.

In Fig. 7 and Fig. 8, the surface temperatures on stator and rotor are compared with measurement data. Also, in this case the qualitative behavior of the measurements is similar to the numerical simulations. The values on the stator are about 2 °C to 3 °C less than the measurements. In the case of the rotor, the values come out about 4 °C too low. The greatest differences on the rotor temperature appear on the fin bases. The thermocouples are located on the fin bases (see Fig. 1) for this reason the locations for the numerical evaluation had to be approximated.

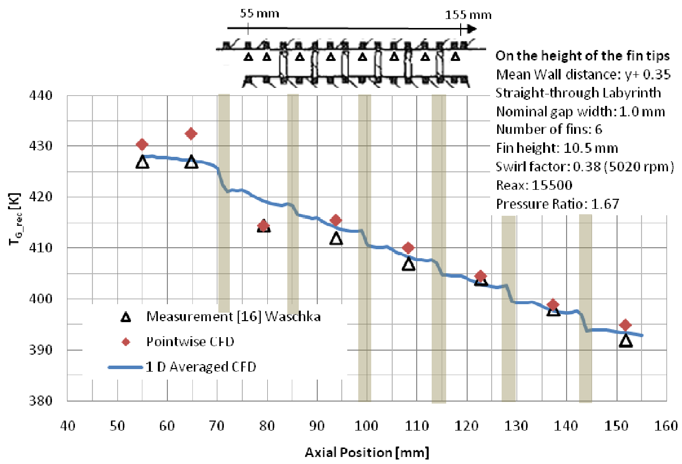

Fig. 6 Comparison of measured gas temperature with CFD values

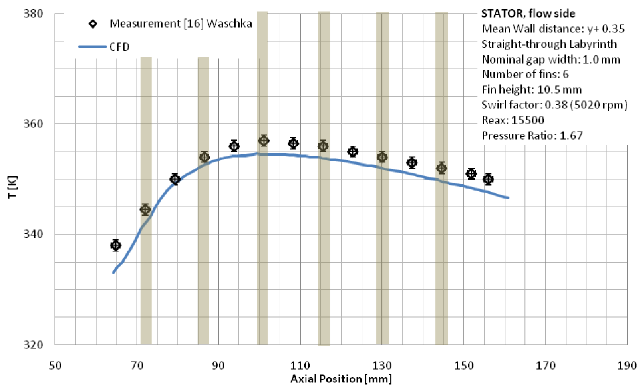

Fig. 7 Comparison of measured surface temperature of the Stator with CFD values

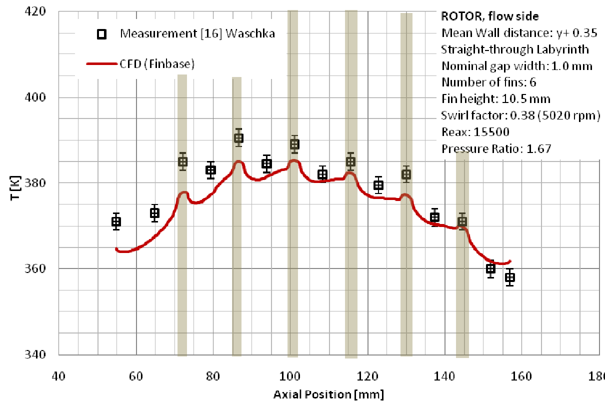

Fig. 8 Comparison of measured surface temperatures of the Rotor with CFD values

Fig. 9 and Fig. 10 show the *local heat transfer* coefficients of the rotor and the stator. On the stator, there is a good agreement between the numerical simulation and the measurements. The values of the simulation are about 10 % too low. The accordance on the rotor is not as good as on the stator, they are about 30 % too low. But again there is a similar curve progression. The relative error range has to be considered due to the temperature measurements. Especially on the rotor, which is cooled with air, the measurement is not as accurate as on the water-cooled stator. Note that a 1 K difference in the temperatures can cause a difference in the heat transfer coefficients of 10 to 15 % (see *Jacobsen [5], 1987*).

So for the case of a very fine mesh, it was possible to achieve a good agreement with the measured data. The higher deviation between test data on the rotor side and numerical results can be partially explained with the measurement uncertainties as indicated by the error bars. On the other side, one has to admit a systematic under prediction of heat transfer coefficients, which has its origins mostly in the insufficiently modeled complex flow structure between the fins.

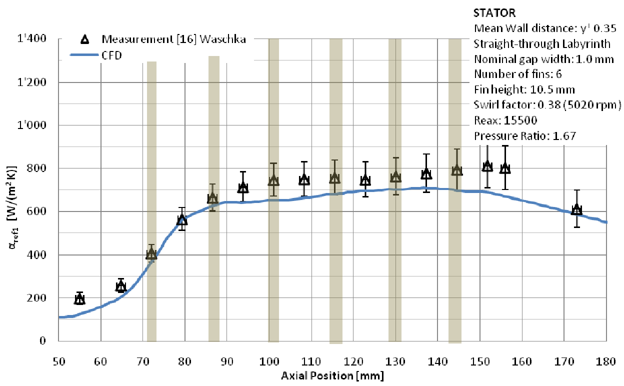

Fig. 9 Local heat transfer coefficients of measurements and CFD data of the Stator

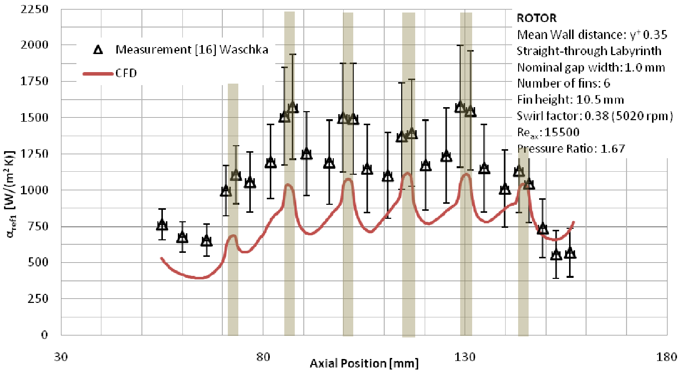

Fig. 10 Local heat transfer coefficients of measurements and CFD data of the Rotor

Influence of Mesh Discretization

One of the most important aspects for numerical simulations is the mesh discretization. Despite the constant development of computer systems and numerical codes, the technical possibilities are still limited. Because of the limitations of technical resources, it is necessary to know how coarse a discretization can be to produce accurate results. A sensitivity analysis shall give an impression of this influence on local and global heat transfer utilizing the meshes that have been presented in Fig. 3.

The first point of interest is the influence of the mesh discretization on the discharge through the labyrinth. Fig. 11 shows that there are no significant differences between the fine and the coarse mesh. But there is another numerical aspect which can cause differences in the discharge. It is the kind of turbulence modeling, which is used. Therefore Fig. 12 illustrates the comparison of the SST-modeling and k-ω-modeling for the finest mesh. The k-ω-model predicts mass flow about 4 to 8 % too low. In contrast the SST-model can reproduce the mass flow quite accurately.

In Fig. 13 and Fig. 14, the local heat transfer behavior of the stator and rotor is illustrated. It has to be noted that for this comparison the definition in equation 4 has been used. One can notice a different behavior between rotor and stator. The impact on the stator turns out clearly less as on the rotor. The average heat transfer, which is displayed in Fig. 15, helps to show this difference in the behavior. A coarse discretization leads to lower heat transfer coefficients in both cases.

On the *stator,* the main differences are located in the first three fins. Especially the local behavior in front of each fin cannot be recognized with a coarse fluid discretization. If a discretization of y+ 50 is used, the distinction of the global heat transfer to y+ 0.3 is only 9 %. The application of numerical wall functions is responsible for this relative small difference of 9 %. These wall functions are an essential part of the turbulence modeling and are able to correct a false temperature development due to coarse mesh discretization at the wall. The contribution of the wall function correction is demonstrated in the Fig. 16 and Fig. 17. In these figures, the temperature distribution in the solid part and the fluid are shown for the different meshes and for a middle position of the rotor and the stator respectively. One can see that the wall temperatures inside the solid domain are only slightly varying, while the wall temperature in the fluid domain deviates increasingly from the solid domain temperature when y+ values exceed 10. The correction of the solid wall temperature is a merit of the wall function, which corrects wall shear stresses and thermal gradients if the resolution is too poor. The corrected values show a mesh dependency of only 2 °C inside the solid domains.

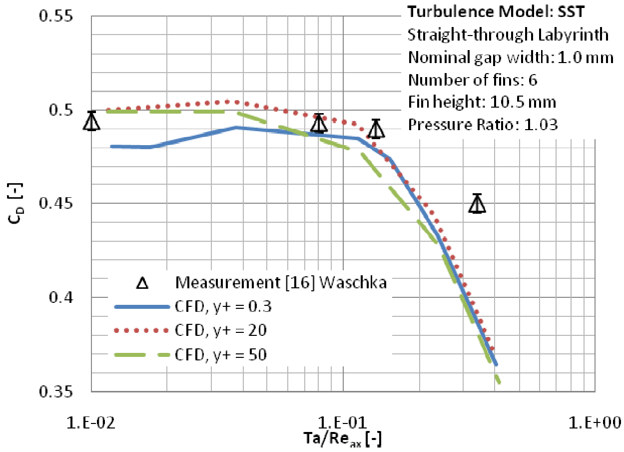

Fig. 11 Influence of mesh discretization on discharge

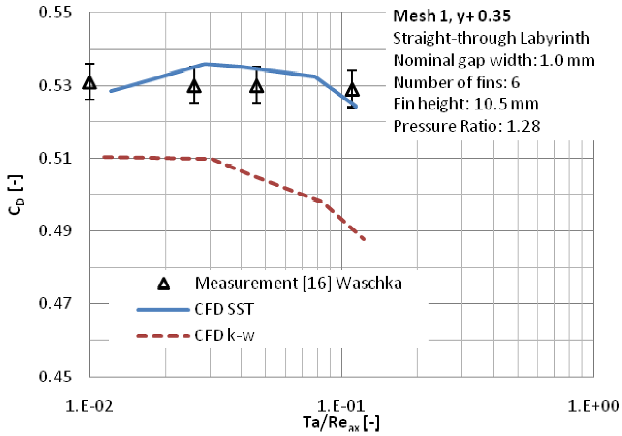

Fig. 12 Influence of turbulence model on discharge

From these figures, it is obvious that only the surface temperatures inside the solid are corrected, and the gas temperature near the surface is still too high. For this reason the choice of reference gas temperatures close to the wall with a coarse mesh has to be considered to be critical. Accordingly the temperature in the wall is, due to the application of wall functions, less dependent on the dimensionless wall distance y^+.

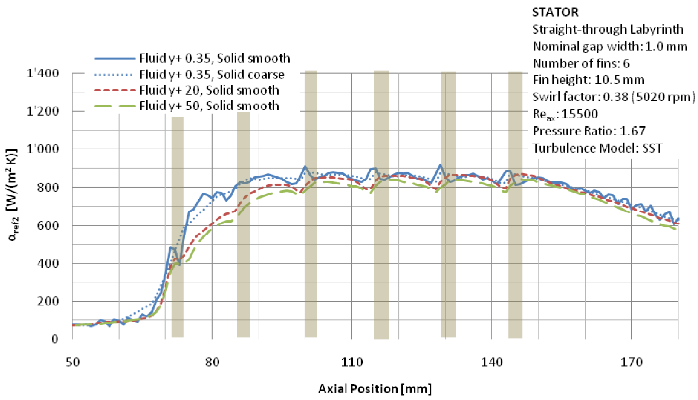

Fig. 13 Influence of the mesh discretization on the local heat transfer coefficients, Stator

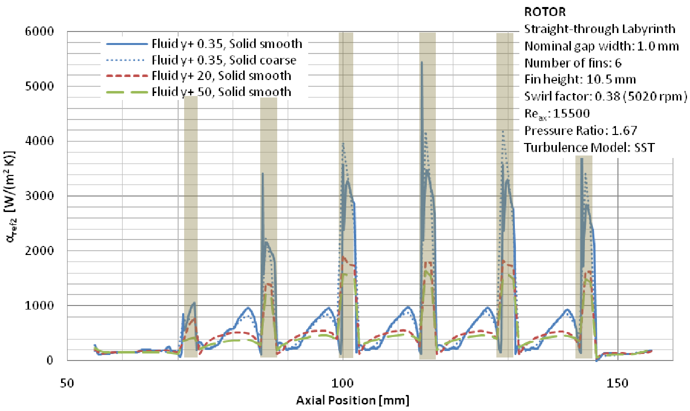

Fig. 14 Influence of the mesh discretization on the local heat transfer coefficients, Rotor

Furthermore the discretization of the *solid domains* does also not noticeably influence the temperature in the solid because the temperature distribution in the metal is rather linear and implies only small discretization errors. The temperature progression in the solid parts is consequently relatively independent from the discretization of the domains if wall functions are used.

In Fig. 15, one can see that the influence of mesh on the *rotor* is far more pronounced despite the influence of wall functions. Predicted local heat transfer coefficients on the fins are about 40 % too low with a coarse mesh, though it is similarly discretized as on the stator mesh. The origin of this deviation is not solely the boundary layer; additionally the flow behavior in the chambers shows differences. In the case of a coarse discretization the distributions of heat transfer (see Fig. 14) is almost symmetric at the bottom of the chambers. In case of the fine meshes there is considerably more non-uniformity in this area. As we have stated that the y^+ seems not to be the only reason, which leads to these differences. Another reason is a bad reproduction of the velocity gradients and prediction of the vortex due to an insufficient discretization inside the flow field.

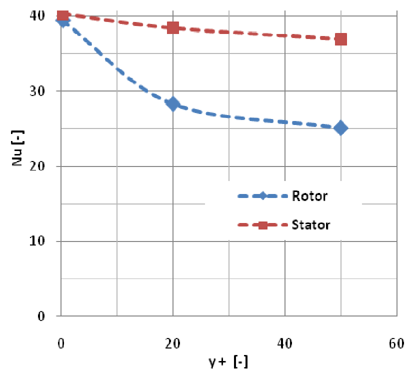

Fig. 15 Influence of the mesh discretization on the global heat transfer with SST Turbulence Modeling

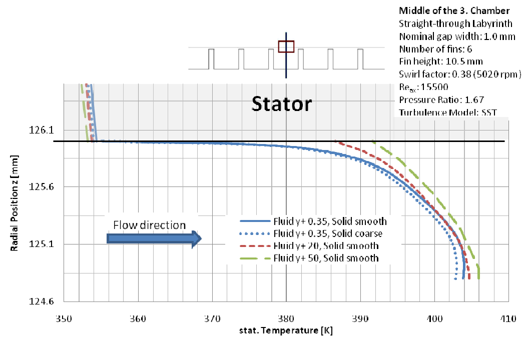

Fig. 16 Influence of the mesh discretization on the near wall temperature in the middle of the 3. Chamber, Stator

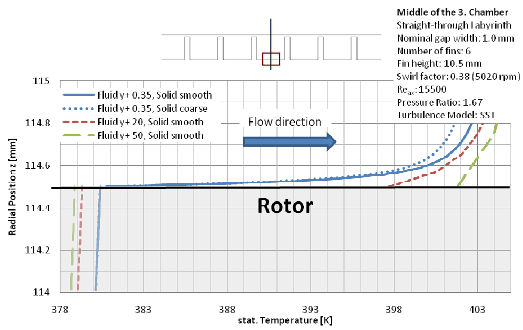

Fig. 17 Influence of the mesh discretization on the near wall temperature in the middle of the 3. Chamber, Rotor

Due to the high number of nodes already used and a sufficient accuracy reached, this grid density is set as reference for further similar applications.

In Fig. 18, the streamlines are compared between the fine and coarse mesh. One can see that the coarse mesh misses details of smaller flow separations in the corners between fin and rotor. The shape of the larger recirculation is affected. This fact leads to a difference in velocity level between mesh 1 and 3. One could see that close to the rotor wall larger differences of more than 30 m/s exist. This indicates differences in wall shear (see Fig. 19) and hence also in heat transfer coefficient.

Because of this, the heat transfer on the rotor, which is influenced by the vortex-system in the chamber, is more sensitive to mesh discretization in the flow field, as the stator. The stator is mainly influenced by the rather 1-dimensional acceleration and deceleration of the flow at the fins, but it experiences little effect of the secondary flow.

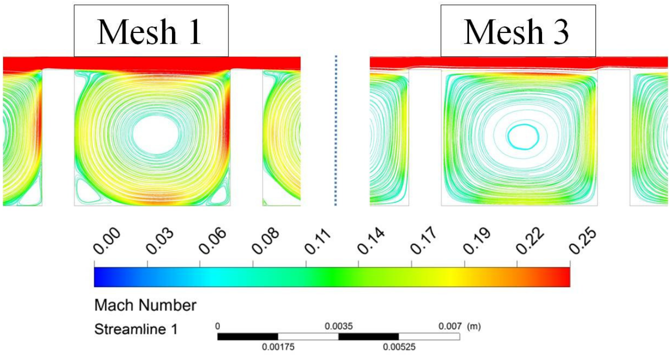

Fig. 18 Velocity streamlines in the chamber, smooth discretization (left), coarse discretization (right)

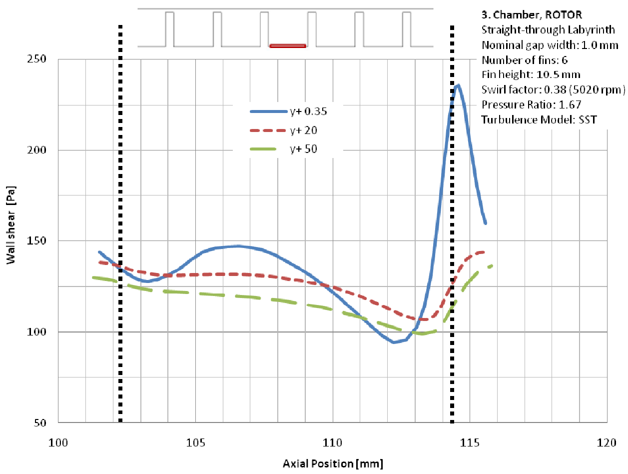

Fig. 19 Influence of mesh discretization on wall shear of the rotor in the 3. Chamber

STEAM TURBINE DESIGN

Fig. 20 gives a schematic view on a typical design of a combined intermediate and low pressure steam turbine module. The intermediate pressure module is derived as a single flow turbine utilizing a piston seal to reduce the leakage from life steam into the combined outer casing.

The lifetime calculation of the rotor depends very much on the static and thermal stresses in the first rotor groove. This area typically limits the cyclic lifetime of the rotor as here the highest stresses occur.

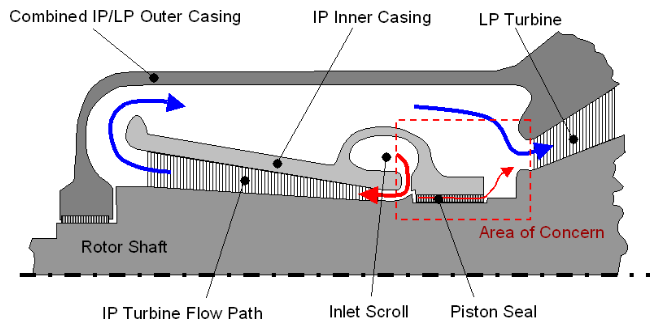

Fig. 20 Typical Alstom combined intermediate-low pressure turbine configuration

In Fig. 21 the area of the piston and the first rotor groove is further detailed schematically. It was found that the thermal load during transient operation is very much influenced by the local heat transfer and temperature in the flow path and labyrinth seal. But also the shape of the labyrinth seal has an influence on the stresses in the rotor.

In this perspective, an innovative design was proposed and developed by Alstom. It considers the introduction of a so called Stress Relief Groove (SRG), a cavity with a shape opportunely optimized with the scope to relieve the stress concentration in the first blade to the cavity. The additional advantage to introduce the groove in the piston seal area is to not degrade the aerodynamic performance of the first stage.

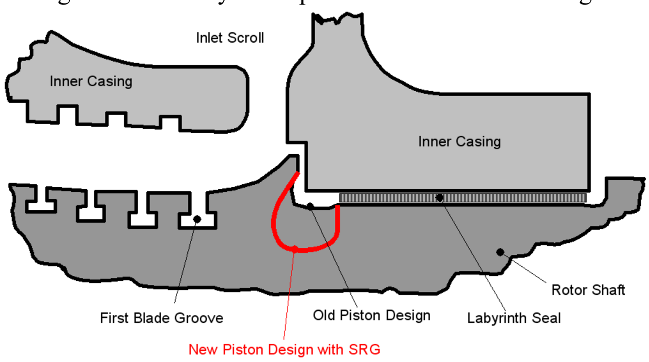

Fig. 21 Stress Relief Groove (SRG) in the Piston seal area

Due to the non-conventional configuration of the piston seal area, a detailed and deep investigation for the definition of reliable thermal boundary conditions inside the groove was necessary, above all to estimate the heat transfer coefficient and temperature distribution in a full transient start-up.
To demonstrate the importance of heat transfer on rotor cyclic lifetime, Fig. 22 shows a sensitivity analysis of HTC values at the outlet of the labyrinth seal on allowable number of warm start-up and shut-down cycles (WS-SD cycles). It is evident as the allowable number of WS-SD cycles at the piston outlet increase with the decrease of HTC in this area.

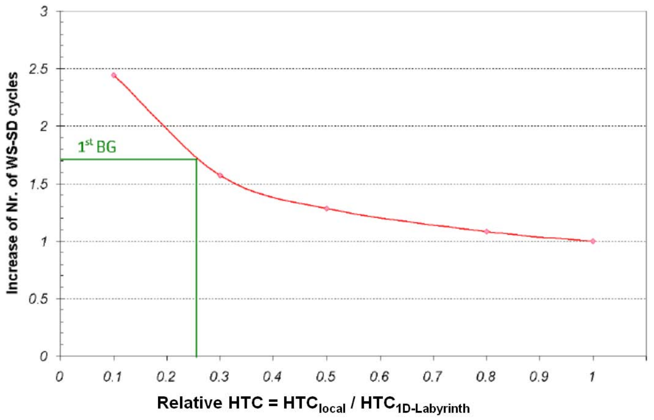

Fig. 22 Influence of HTC on the allowable number of WS-SD cycle at the piston outlet

For this reason, a full coupling CHT (Conjugate Heat Transfer) analysis was carried out on the piston and labyrinth seal to simulate accurately the heat transfer behavior on the rotor. The numerical model is based upon the findings from the experimental validation case of the previous chapter. This especially includes best practices for the mesh generation and turbulence model.

These information (HTC and steam temperature) are then transferred to a well assessed and validated tool for life time estimation, developed by Alstom, taken in account an appropriate safety margin factor and the precision of the numerical approach as detected in the previous investigation.

LIFE TIME ASSESSMENT

CHT model configuration

Fig. 23 illustrates the computational domain for the CHT simulation. Part of the inner casing, rotor and the entire piston seal area were resolved simultaneous to couple the heat fluxes between the fluid and solid region. A sector computation is performed with axi-symmetric condition, with one cell in circumferential direction. The fluid domain is based on the wheel chamber (after the radial stage and before the first rotor blade), the stress relief groove and the labyrinth seal. The labyrinth seal includes more then 60 fins and is of a double-labyrinth type with same number of alternating fins on the rotor and stator side with equal tip clearance.

Part of the wheel chamber is included in the computation in order to have a better estimation of the flow swirl at the inlet of the sealing, because it can affect the windage contribution.
The mesh is generated using ICEM CFD 12.1. The entire fluid domain is discretized using hexahedral element with 2.4 million nodes, respecting the mesh density of the previous assessment in order to insure the grid independency of the solution. The mesh is very well refined at the wall to insure a y+ value close to 1 inside the groove. The solid domain has tetrahedral element with 300,000 nodes. The turbulence model chosen for this simulation is the SST, which allows the resolution of the laminar sublayer without wall functions, that is evaluated as an effective turbulence model for heat transfer problems (see [1]).

The commercial package ANSYS CFX 12.1 is used to resolve the flow. As boundary conditions typical parameters for a steam turbine are applied for the total pressure P_0, total temperature T_0 and swirl angle at the inlet of the domain, and the static pressure P_{exit} at the outlet of the labyrinth seal. The velocity of the rotor is 3000 [rev / min]. The real steam table IAPWS 97 are applied in the simulation.
The boundary conditions for the solid domain are defined in terms of steam temperature and heat transfer coefficient at the outer boundaries of the solid domains.

Results

Fig. 23 shows the temperature contour plot distribution on the entire domain, inner casing, rotor and fluid domain, in particular on the groove.

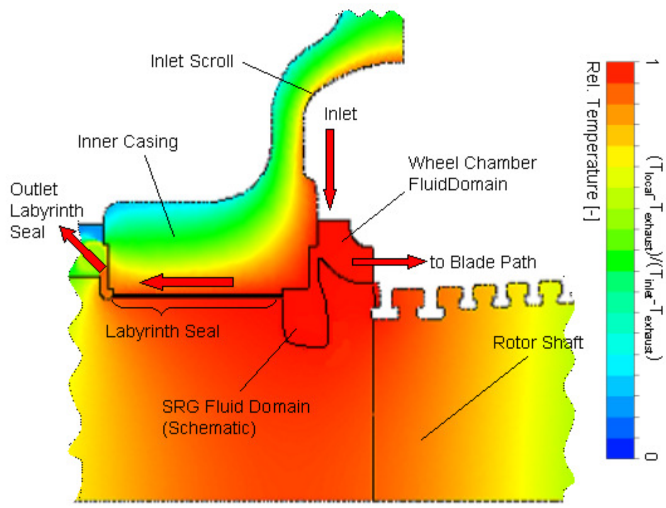

Fig. 23 Temperature contour. Inner Casing, rotor and fluid domain

The heat transfer coefficient in the groove is conventionally defined as per equation 4 where Ts is the wall temperature on the rotor surface and T_{G_ref2} is the temperature at the inlet of the seal.

Fig. 24 shows the Mach Number contour plot with surface streamlines. One can see that the leakage flow entering the SRG is concentrating as a jet that leaves several separation and recirculation bubbles inside the cavity before it leaves through the labyrinth seal.

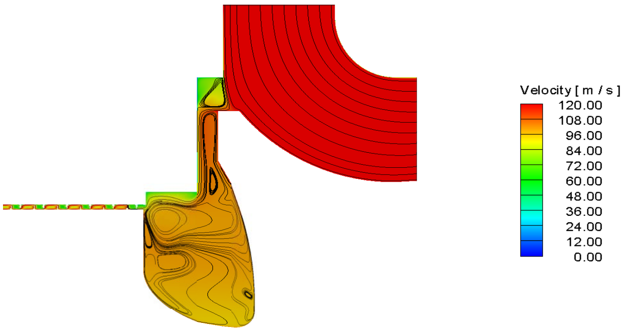

Fig. 24 Mach Number contour inside the groove (schematic contour)

LIFETIME RESULTS

A well assessed and automated process to compute the whole start-up simulation of a steam turbine was build up by Alstom (see Hardee and Ehrsam [4]).

The flow chart of the entire procedure is illustrated in Fig. 25, where an iterative loop is performed with the interlink of Abaqus FEA from SIMULIA, for the stress analysis, and an Alstom's in-house thermodynamic code for the generation of the boundary conditions. The temperatures and HTC at labyrinth seal in the thermodynamic program have been calibrated based on the results of the CHT study described in the earlier chapter. In this way the results of the CHT study could be integrated into the lifetime calculation. In the following the tool was used to determine optimal transient thermal boundary conditions based on real-time thermal stresses and automated the search for optimal process parameters through the use of a feedback control algorithm.

At the beginning of the loop, the Alstom thermodynamic program generates the thermal boundary conditions for the first time-increment. Abaqus then calls a subroutine to apply the thermal boundary condition to the model of the turbine rotor, and to complete the first time increment of the thermo-mechanical analysis.

For the next time-increment, Abaqus first extracts the actual stresses at critical locations from its output database, calls the control algorithm to determine the optimal mass flow, then queries the Alstom code for the thermal boundary conditions based on this information, and finally performs the subsequent time-increment of the thermo-mechanical analysis. This computational loop is repeated for each time-increment, comparing the computed stresses at critical locations with the material stress limits.

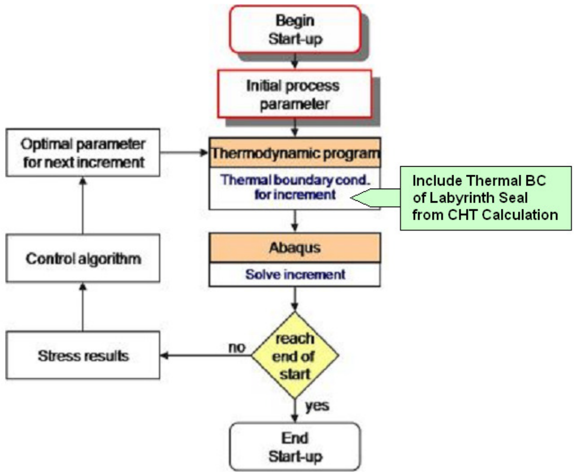

Fig. 25 Automated start-up parameter optimization flow chart with in-house thermodynamic code and Abaqus FEA

The optimization has lead to the so-called Stress Relief Groove (SRG) demonstrated in Fig. 21, which has lead to about double of the lifetime of the conventional design.

CONCLUSIONS

With a correct application, actual codes are able to reproduce complex physical phenomena. In this conjugate heat transfer problem the numerical model could reproduce the temperature distributions with maximal differences of 4 K in comparison with measurement data. Due to the validated temperature results, also the local heat transfer behavior can be trusted. The differences to measurements count about 10 % in the case of the stator and about 30 % for the rotor. In the context of this work and general insecurity of local heat transfer values these differences are acceptable.

The main influence parameter on the simulation results is the mesh discretization of the domains. In the case of the solid domains it is not very important, but especially in the fluid domain. But not only the near wall discretization, the so-called dimensionless wall distance, also the discretization in the flow field at positions of important flow forms is important. A bad near wall discretization can mostly be corrected with the usage of actual wall functions. This fact can be seen on the stator, whose heat transfer changes only 9 % with a y+ of 50 in comparison to the complete discretization of the viscous boundary layer. However the rotor, whose heat flux is more dependent on sensitive flow-forms (swirls, strong gradients) needs a smooth enough discretization of the flow field.

Results of CHT study made a substantial contribution to the development of novel designs of labyrinth seals, which helped to increase steam turbine rotor lifetime by more than 100%.

ACKNOWLEDGMENTS

The authors would like to thank Mr Thomas Schreier and Mr. Andreas Ehrsam for the review of the material and their kind support on questions regarding lifetime calculations and thermal stress.

REFERENCES

[1] Bardina, J.E., Huang, P.G. and Coakley, T.J., (1997) "Turbulence Modeling, Validation, Testing and Development", NASA Technical Memorandum 110446. (See also Bardina, J.E., Huang, P.G. and Coakley, T., "Turbulence Modeling Validation," AIAA Paper 97-2121)

[2] Demeulenaere A., Bonaecorsi J-Ch., Patel A. and Hirsch Ch., (2005), "Application of an unstructured Flow Solver to the Calculation of Conjugate Heat Transfer Problems in Turbine Blades", Proceedings of the 6th European Conference on Turbomachinery, Fluid Dynamics and Thermodynamics, March 7-11, Lille, France, pp. 854-863.

[3] Egli, A. (1935), "The leakage of steam through labyrinth seals", Trans. ASME 57, S.FSB-115/22; Discussion: Trans. ASME 57 (1935), S. 445/46.

[4] Hardee C. and Ehrsam A., (2010) "Fast Starts Help Squeeze Watts", Article in Power-Gen Worldwide, May 18.

[5] Jacobsen, K. (1987), "Experimentelle Untersuchungen zum Durchfluss und Wärmeübergang in Durchblick- und Stufenlabyrinthdichtungen", Dissertation, Institut für Thermische Strömungsmaschinen der Universität Karlsruhe

[6] Jones, J.S. (1952), Discussion about [7], Proc. Inst. Mech. Engrs. 166, S. 180/88.

[7] Kearton, W.J. and Keh, T.H. (1952), "Leakage of air through labyrinth glands of staggered type", Proc. Instn. Mech. Engrs. 166, S. 180/88.

[8] Komotori, K. (1961), "Probleme bei Labyrinth-Stopfbüchsen", Proc. oft the Fujihara Memorial Faculty of Engng., Keio University Japan, Vol. 14, Nr. 54, S.1/48.

[9] Komotori, K. and Miyake, K. (1977), "Leakage characteristics of labyrinth seals with high rotating speed", Proc. 1977; Tokyo Gas Turbine Congress, S. 371/80

[10] Mokulys T., Ferrari F., Haertel C. and Abhari R.S, (2003) "Uncertainty analysis of Predicted Heat Transfer for Turbomachinery Flows", Proceedings of the Conference of Modelling Fluid Flow, September, CMFF, Budapest.

[11] Rhode, D.L. and Sobolik, S.R. (1986) "Simulation of subsonic flow through a generic labyrinth seal", Trans-ASME, October, Vol.108.

[12] Rzadkowski R., Lampart P., Kwapisz L., Szymaniak M. and Drewczynski M., (2010) "Transient Thermodynamic, Thermal and Structure Analysis of a Steam Turbine During its Startup", Proceedings of ASME Turbo Expo 2010, GT2010-22813.

[13] Scherer, T. (1994) "Grundlagen und Voraussetzungen der numerischen Beschreibung von Durchfluss und Wärmeübergang in rotierenden Labyrinthdichtungen", Dissertation, Institut für Thermische Strömungsmaschinen der Universität Karlsruhe

[14] Stodola, A. (1927), Dampf- und Gasturbinen

[15] Trutnovsky K. and Komotori K. (1981), "Berührungsfreie Dichtungen", VDI-Verlag, Düsseldorf.

[16] Waschka, W. (1991), "Zum Einfluss der Rotation auf das Durchflussverhalten und Wärmeübertragungsverhalten in Labyrinthdichtungen und Wellendurchführungen", Dissertation, Institut für Thermische Strömungsmaschinen der Universität Karlsruhe.

